ALMOST RECTILINEAR HALO ORBITS

K. C. HOWELL* and J. V. BREAKWELL
Dept. of Aeronautics and Astronautics, Stanford University,
Stanford, CA 94305, U.S.A.

(Received 1 June, 1982; accepted 8 July, 1983)

ABSTRACT. Numerical studies over the entire range of mass-ratios in the circular restricted 3-body problem have revealed the existence of families of three-dimensional 'halo' periodic orbits emanating from the general vicinity of any of the 3 collinear Lagrangian libration points. Following a family towards the nearer primary leads, in 2 different cases, to thin, almost rectilinear, orbits aligned essentially perpendicular to the plane of motion of the primaries.
(i) If the nearer primary is much more massive than the further, these thin L_3-family halo orbits are analyzed by looking at the in-plane components of the small osculating angular momentum relative to the larger primary and at the small in-plane components of the osculating Laplace eccentricity vector. The analysis is carried either to 1st or 2nd order in these 4 small quantities, and the resulting orbits and their stability are compared with those obtained by a regularized numerical integration. (ii) If the nearer primary is much less massive than the further, the thin L_1-family and L_2-family halo orbits are analyzed to 1st order in these same 4 small quantities with an independent variable related to the one-dimensional approximate motion. The resulting orbits and their stability are again compared with those obtained by numerical integration.

1. INTRODUCTION

Previous papers have presented three-dimensional, periodic 'halo' orbits found in the restricted, 3-body problem. Farquhar and Kamel (1973) first predicted and found halo orbits near the translunar L_2 libration point in the Earth-Moon system. Breakwell and Brown (1979) then extended these into an L_2 family of orbits. They also found and computed a family originating near the L_1 libration point between the Earth and the Moon. Of particular interest, stable orbits were found in each family. From these results, additional families were calculated for various mass ratios (Howell, 1984). Mass ratios both larger and smaller than that for the Earth-Moon case of μ=0.012 were used. This also permitted calculation of halo orbits near L_3, on the far side of the Earth. Stable three-dimensional orbits were found

* Present address: School of Aeronautics and Astronautics, Purdue University, West Lafayette, IN 47907, U.S.A.

Celestial Mechanics **32** (1984) 29-52. 0008-8714/84/0321-0029 $03.60.

in the majority of cases. In both the L_2 and L_3 cases, the families tend toward almost rectilinear orbits as the initial point moves closer to the nearest primary. Breakwell and Brown presented an 'analytical' approximation to these orbits in the L_2 family. The almost rectilinear orbits constituted in fact a kind of bridge between the L_2 family and the L_1 family. The approximation produced linear non-homogeneous equations to calculate position and velocity as well as indicate stability.

2. ANALYSIS

2.1. Problem Definition

The circular restricted three-body problem involves the two finite masses m_1 and m_2, assumed to be point masses, moving in circles around their common mass center, each under the gravitational influence of the other. A rotating coordinate system, with origin at m_2 is chosen. μ is defined as the mass ratio m_2 to the sum m_1+m_2.

The system is shown in Figure 1 as it would appear for $\mu>0.5$.

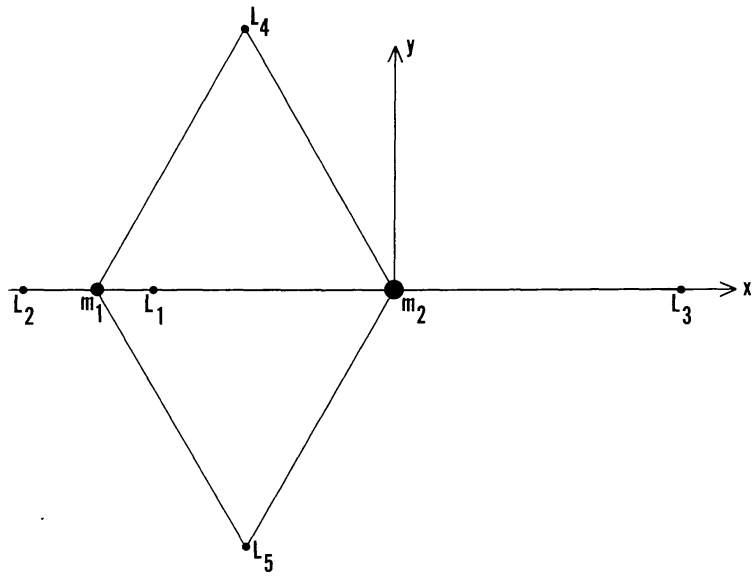

Fig. 1. Libration points.

The x-y plane is the plane of motion of the masses m_1 and m_2. A z-axis out of the page completes the right-handed system. The third body, m_3, is assumed massless but may travel in three dimensions. The five equilibrium, or libration, points are shown. For convenience, nondimensional units were used such that the sum of the masses, m_1+m_2, is equal to 1, the distance between the primaries is equal to 1, and the angular velocity of the x-axis equals 1. The equations of motion are

$$\begin{aligned} \ddot{x} - 2\dot{y} &= \frac{\partial U}{\partial x}, \\ \ddot{y} + 2\dot{x} &= \frac{\partial U}{\partial y}, \\ \ddot{z} &= \frac{\partial U}{\partial z}, \end{aligned} \tag{2.1}$$

where

$$U = \frac{1}{2}(x^{*2} + y^2) + \frac{1-\mu}{d} + \frac{\mu}{r},$$

$$x^* = x + 1 - \mu,$$

d = distance from m_1,

r = distance from m_2,

Dots denote d/dt. The equations are known to yield a constant of integration, C, given by

$$\frac{\dot{x}^2 + \dot{y}^2 + \dot{z}^2}{2} = U - \frac{C}{2}. \tag{2.2}$$

Also needed is the 6x6 transition matrix, $\Phi(t, 0)$, of partial derivatives, $\partial X(t)/\partial X(0)$. X is a column vector with elements x, y, z, $\dot{x}$, $\dot{y}$, $\dot{z}$. Here $\Phi(0, 0) = I$, the identity matrix and

$$\frac{d}{dt}\Phi(t, 0) = A(t)\Phi(t, 0), \tag{2.3}$$

where

$$A(t) = \left(\begin{array}{c|c} 0 & I \\ \hline U_{XX} & 2\Omega \end{array}\right).$$

$$\Omega = \begin{pmatrix} 0 & 1 & 0 \\ -1 & 0 & 0 \\ 0 & 0 & 0 \end{pmatrix}.$$

and U_{XX} is the symmetric matrix of second partial derivatives of U with respect to x, y, z, evaluated along the orbit. The values of Φ at a recrossing of the x-z plane are used to assist (see Breakwell and Brown, 1979) the convergence toward an orbit with a second perpendicular crossing of the x-z plane, i.e., a periodic orbit. Stability is determined by the eigenvalues of the full-cycle transition matrix $\Phi(t_F, 0)$. Two of the eigenvalues are always 1. The other four are in reciprocal pairs $(\lambda_i, 1/\lambda_i)$, since the equations are invariant under $t \to -t$, $y \to -y$. The 6x6 matrix $\Phi(t_F, 0)$ can be reduced as shown in Breakwell and Brown (1979) and Howell (1981) to a 4x4 matrix $\mathfrak{M}$ to produce the 4 critical eigenvalues. Two stability indices have been defined as the arithmetic mean of each pair, $\nu_i = 1/2(\lambda_i + 1/\lambda_i)$.

The stability indices can be calculated directly (see Broucke, 1969) from

$$\nu = \tfrac{1}{2}[\operatorname{tr}\mathfrak{M} \pm \sqrt{8 + 2\operatorname{tr}(\mathfrak{M}^2) - (\operatorname{tr}\mathfrak{M})^2}]. \tag{2.4}$$

Stability requires <u>real</u> ν's between -1 and +1.

Planar projections of selected members of the family of halo orbits found near L_3 for μ=0.96 are shown in Figures 2a-b. The value $x^*=x+1-\mu$ and is the distance from the barycenter in the x-direction. The x-z projections

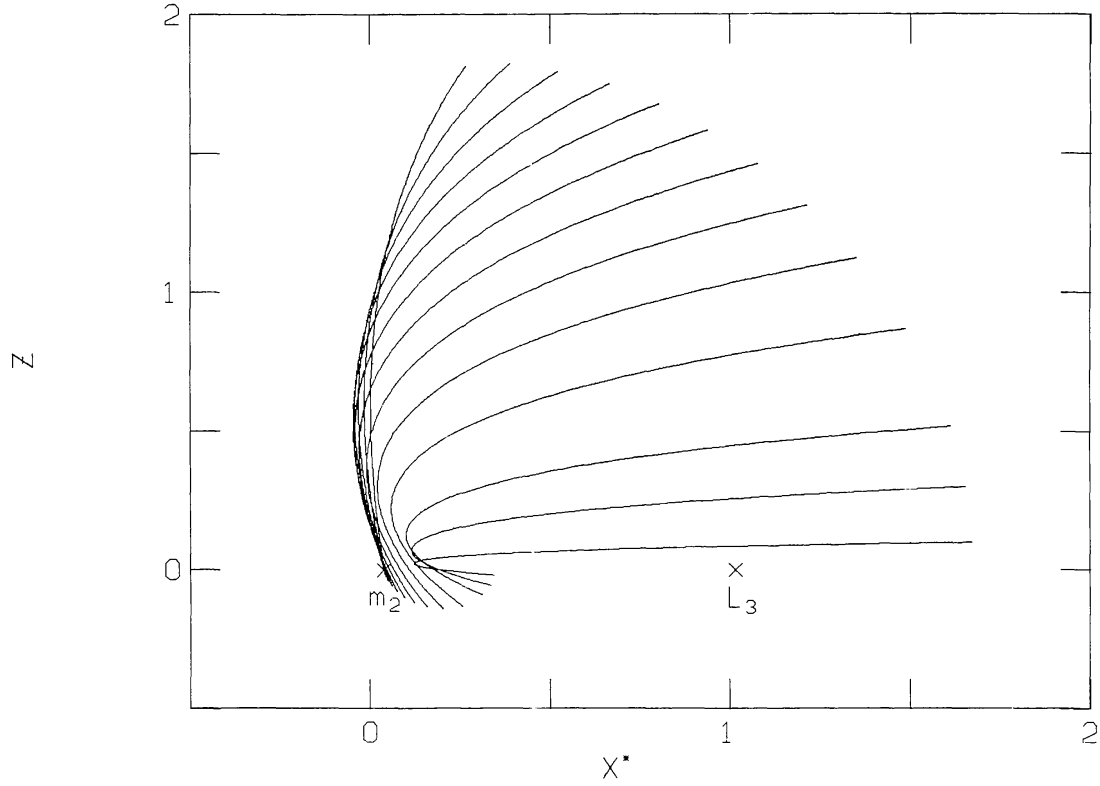

Fig. 2a. x-z projection, L_3 family, μ=0.96.

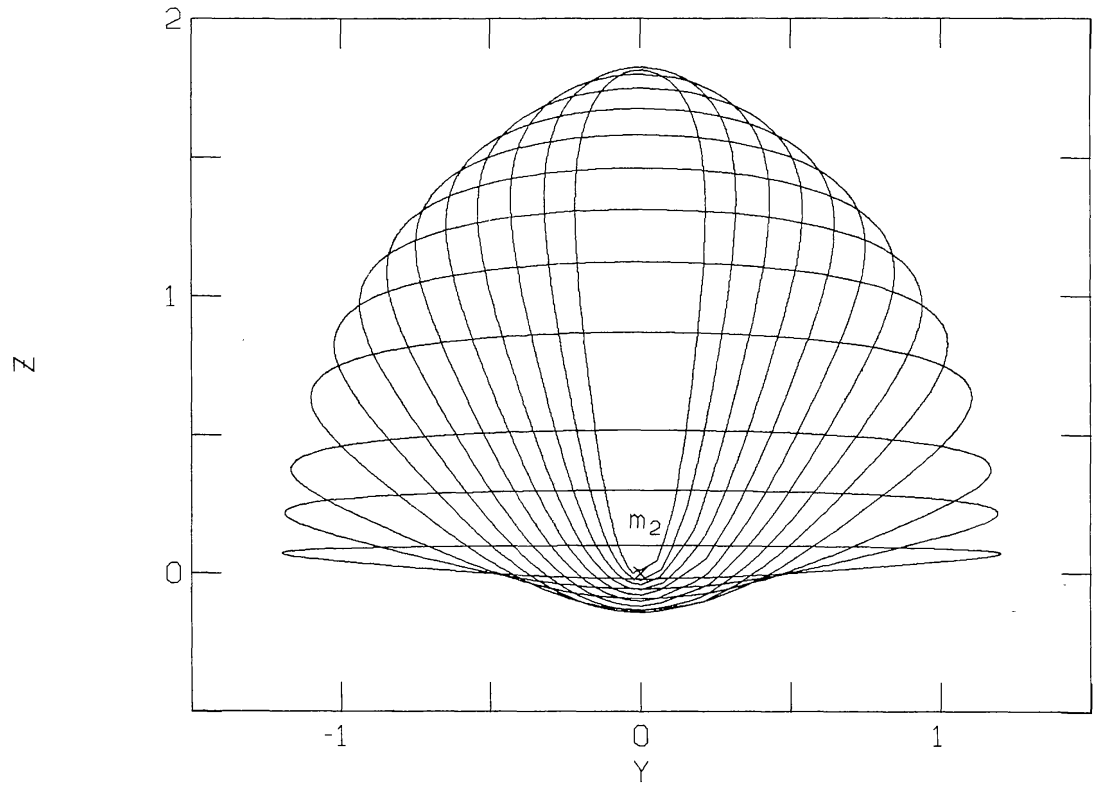

Fig. 2b. y-z projection, L_3 family, μ=0.96.

are shown in Figure 2a. It can be seen that the point with the maximum x and maximum z value is unique for each orbit. For that reason, the x_{max} value is used to identify each member of the family. It can be seen in the two plots that the family is tending toward orbits which have a large out-of-plane component (z) and increasingly smaller in-plane components. They also appear to be approaching a collision with m_2.

2.2. Integration Scheme

One of the main difficulties involved in the results shown thus far is the third body moving toward a close approach with the nearer mass. The singularities of the differential equations, notably in the potential U (i.e., $\partial U/\partial x_i$) and in the equations for the transition matrix result in a considerable increase in computer time and serious accuracy problems. The singularities can be eliminated by using a regularization transformation.

The method employed for three-dimensional regularization developed from that presented by Kustaanheimo and Stiefel (1965) for Kepler motion. Bettis and Szebehely (1971) discussed the numerical approaches in considerable detail.

Regularization in the three-dimensional space R^3 involves a simple mapping of a four-dimensional space R^4 onto R^3. In R^4 the equations remain completely regular at the center of the chosen primary. In the restricted three-body problem, singularities occur at both primaries. This paper is concerned only with close approaches to one of these masses.

To remove the singularity when r becomes small, it is necessary to introduce both a coordinate transformation and a transformation of the independent variable. The transformation of the time, t, is

$$dt = r\, d\tau. \tag{2.5}$$

The new independent variable, τ, was used in the equations to produce most of the results in Figures 2a-b. It facilitated a smoother and more efficient change in step size. For the coordinate transformation, Kustaanheimo and Stiefel introduce two four-dimensional column vectors, $\bar{R}$ and the new variables in $\bar{u}$, which are related by

$$\bar{R} = \mathfrak{L}(\bar{u})\bar{u}, \tag{2.6}$$

where

$$\bar{R} = (x, y, z, 0)^T,$$
$$\bar{u} = (u_1, u_2, u_3, u_4)^T,$$
$$\mathfrak{L}(\bar{u}) = \begin{pmatrix} u_1 & -u_2 & -u_3 & u_4 \\ u_2 & u_1 & -u_4 & -u_3 \\ u_3 & u_4 & u_1 & u_2 \\ u_4 & -u_3 & u_2 & -u_1 \end{pmatrix}.$$

Superscripts T denotes transpose. Recall that the equations of motion in R^3 are in the rotating coordinate system and appear as written in (2.1). The equations in R^4 in the variables u_i are produced from these. In matrix notation, they are:

$$\bar{u}'' - \frac{h}{2}\bar{u} = \Omega^T(\bar{u})\bar{\bar{B}}\Omega(\bar{u})\bar{u}' + \frac{(\bar{u}\cdot\bar{u})}{2}\Omega^T(\bar{u})\bar{F}, \tag{2.7}$$

where

$$\bar{\bar{B}} \quad \begin{pmatrix} 0 & 2 & 0 & 0 \\ -2 & 0 & 0 & 0 \\ 0 & 0 & 0 & 0 \\ 0 & 0 & 0 & 0 \end{pmatrix}, \qquad \bar{F} = \begin{pmatrix} -\frac{(1-\mu)(1+x)}{d^3} + x^* \\ -\frac{(1-\mu)y}{d^3} + y \\ -\frac{(1-\mu)z}{d^3} \\ 0 \end{pmatrix}.$$

Prime indicates differentiation with respect to τ, the new independent variable. Very significant in eliminating the singularity is the quantity

$$h = \frac{2(\bar{u}'\cdot\bar{u}')}{(\bar{u}\cdot\bar{u})} - \frac{\mu}{r} = \frac{(1-\mu)}{d} + \frac{1}{2}(x^{*2} + y^2) - \frac{C}{2}. \tag{2.8}$$

The constant C is evaluated from Equation (2.2) at the initial time. Note that $(\bar{u}\cdot\bar{u})=r$. (See Appendix A for details of the derivation.)

For the transition matrix, $\Phi(t, 0)$, it is not sufficient to simply transform the differential equation. It contains r^5 in the denominator and the coordinate transformation could not completely remove the problem. Instead the 8x8 transition matrix associated with the u's is calculated. The resulting equations contain no singularities. It is used at $t_F/2$ to help convergence toward a periodic orbit. Then at t_F, the full-cycle 8x8 matrix can be reduced to the desired 4x4 $\mathfrak{M}$ matrix needed to indicate stability where

$$\begin{pmatrix} dx_F \\ dz_F \\ d\dot{x}_F \\ d\dot{z}_F \end{pmatrix} = \mathfrak{M} \begin{pmatrix} \delta x_0 \\ \delta z_0 \\ \delta \dot{x}_0 \\ \delta \dot{z}_0 \end{pmatrix}. \tag{2.9}$$

(See Appendix A for the derivation of $\mathfrak{M}$.)

A disadvantage of this method is that there are now 73 differential equations and they are much more complicated (requiring more computations) than the original 42 or 43. This is generally offset, however, by the fact that they can be used in regions where the original equations were unsatisfactory. In some regions where the original equations were used successfully, the regularized equations may use a stepsize 2 or 3 orders of magnitude larger than the original set - many more computations per integration step, but many times fewer the number of steps.

Any long integration scheme, however, takes much computer time and stepping along a halo family is slow - small jumps from one orbit to the next to successfully converge. The next section will be devoted to discussing an analytic approximation to those orbits which pass close to the nearer primary.

3. APPROXIMATION FOR THE L_3 FAMILIES

The orbits near the mass in the L_3 case are characterized by the fact that, except near close approach, $x, y \ll z$. The first and second order approximate approaches developed are based on that assumption. An example of the orbit being approximated appears in Figure 3.

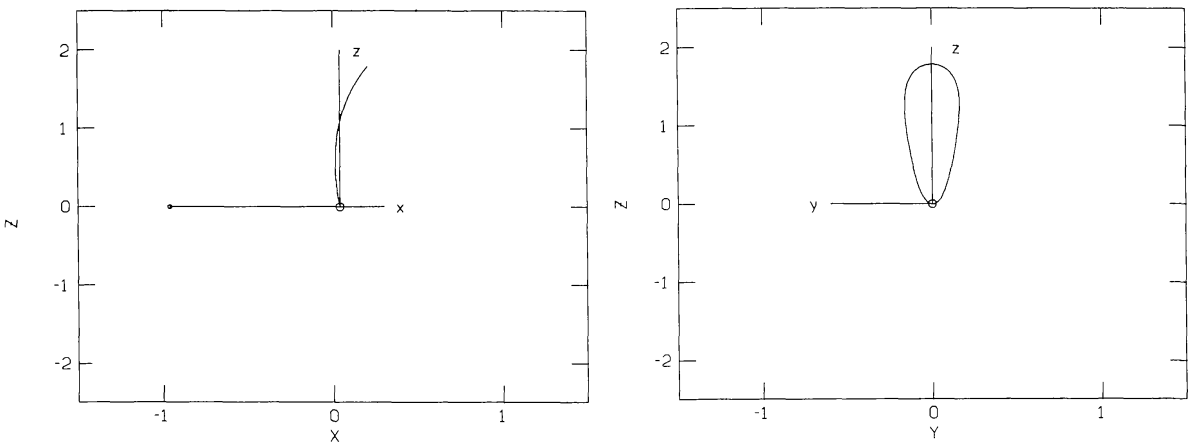

Fig. 3. Halo orbits in L_3 family.

The orbits are very close to the larger mass. The distance from m_2 is given by r, with the x value changing very little during one period. It can be modelled as a perturbed Kepler orbit.

The vector V is denoted $\bar{V}$. A unit vector in the same direction as $\bar{V}$ is written $\hat{V}$. Then, with the definition of the constant

$$a = \tfrac{1}{2} r_{max},$$

position in the orbit from the large mass at a given time can be written as

$$\bar{r} \cong a(1 - \cos E)(-\bar{e}) + \hat{z} \times \bar{h} \sqrt{\frac{a}{\mu}} \sin E, \tag{3.1}$$

where

E = eccentric anomaly ($E = \pi$ at r_{max});

$\bar{e}$ = Laplace's eccentricity vector = $\dfrac{\bar{V} \times \bar{h}}{\mu} - \hat{r}$;

$\bar{h}$ = angular momentum vector = $\bar{r} \times \bar{V}$;

$\bar{V}$ = velocity as seen in the non-rotating frame.

To aid in determining the effect of the smaller mass choose the small parameter $\varepsilon = m_1/(m_1+m_2) = 1-\mu$.

To produce both a 1st order and a 2nd order approximation, the following definitions are used, truncated to 2nd order,

$$\bar{e} \cong e_x \hat{x} + e_y \hat{y} - (1 - \varepsilon^2 e_z^{(2)})\hat{z}, \tag{3.2}$$
$$\bar{h} \cong h_x \hat{x} + h_y \hat{y},$$

where

$$e_\alpha = \varepsilon e_\alpha^{(1)} + \varepsilon^2 e_\alpha^{(2)}, \quad \alpha = (x, y),$$
$$h_\alpha = \varepsilon h_\alpha^{(1)} + \varepsilon^2 h_\alpha^{(2)}, \quad \alpha = (x, y),$$

both of which are small. The superscripts (1) and (2) indicate 1st and 2nd order terms. Finally the presence of the mass m_1 will not only disturb the position of m_3 from that in a 2-body Kepler orbit, it will also make a time correction necessary. To produce a differential equation for the correction to the time, start with the mean anomaly M. It can be approximated here as M=E-sin E. M is also defined in terms of the mean motion n as nt=M with t measured from periapsis. Because of the perturbation this is no longer strictly true. If the first order correction is defined to be Δ, a function of M, it can be rewritten

$$nt \cong M + \varepsilon\Delta(M), \tag{3.3}$$

where

$$n = \sqrt{\mu/a^3},$$

which is truncated to first order. The first order equation of motion is used to determine the time correction.

$$\ddot{r} = -\frac{n^2a^3}{r^2} + f_r. \tag{3.4}$$

To rewrite the left side of the equation, differentiate the first order form r=a(1-cos E) with respect to time (noting that $\dot{E}=\dot{M}/(1-\cos E)$) to produce

$$\dot{r} = \frac{a \sin E}{1 - \cos E}\,\dot{M}. \tag{3.5}$$

Find $\dot{M}$ by differentiating (3.3) such that

$$\dot{M} = \frac{n}{1 + \varepsilon\Delta'}, \tag{3.6}$$

where prime indicates differentiation with respect to M. Then (3.5) appears as

$$\dot{r} = \frac{a \sin E}{1 - \cos E}\, n(1 + \varepsilon\Delta')^{-1}. \tag{3.7}$$

Differentiating (3.7) again with respect to time, substituting (3.6) and dropping higher order terms results in

$$\ddot{r} = -\frac{n^2a}{(1 - \cos E)^2}(1 - 2\varepsilon\Delta') - \frac{n^2a \sin E}{(1 - \cos E)}\varepsilon\Delta''. \tag{3.8}$$

On the right side of Equation (3.4), f_r is the perturbing force in the r direction. The total perturbing force due to m_1, written in nondimensional variables, is

$$\bar{f}_1 = (1 - \mu)\left[\hat{x} - \frac{(\hat{x} + \bar{r})}{|\hat{x} + \bar{r}|^3}\right]. \tag{3.9}$$

So the needed approximation is

$$f_r \cong -\frac{\varepsilon n^2a^4(1 - \cos E)}{[1 + a^2(1 - \cos E)^2]^{3/2}}. \tag{3.10}$$

Substituting (3.8), (3.10) and r=a(1-cos E) into (3.4) and rearringing produces a differential equation for the time correction Δ,

$$\Delta'' - \frac{2}{(1 - \cos E)\sin E}\Delta' = \frac{(1 - \cos E)^2}{\sin E\left[\left(\frac{1}{a}\right)^2 + (1 - \cos E)^2\right]^{3/2}} . \quad (3.11)$$

The other differential equations for the system can be derived from

$$\dot{\bar{h}} = \bar{r} \times \bar{f}_1,$$
$$\dot{\bar{e}} = (1/\mu)[\bar{f}_1 \times \bar{h} + \bar{V} \times (\bar{r} \times \bar{f}_1)]. \quad (3.12)$$

The Equations (3.12) can be reduced to produce 1st and 2nd order terms separately for angular momentum and eccentricity. The resulting equations are

$$\begin{aligned}
h_x^{(1)'} &= K^{3/2} h_y^{(1)}, \\
h_y^{(1)'} &= -K^{3/2} h_x^{(1)} + \gamma, \\
h_x^{(2)'} &= K^{3/2} h_y^{(2)} + K^{3/2}\beta h_y^{(1)} \\
h_y^{(2)'} &= -K^{3/2} h_x^{(2)} - K^{3/2}\beta h_x^{(1)} + K^{5/2}(1 - \cos E)B_2 h_y^{(1)} - \\
&\quad - K^{5/2}(1 - \cos E)B_1 e_x^{(1)} + \gamma\beta, \quad (3.13) \\
e_x^{(1)'} &= K^{3/2} e_y^{(1)} - K^2 \sin E(1 - A), \\
e_y^{(1)'} &= -K^{3/2} e_x^{(1)}, \\
e_x^{(2)'} &= K^{3/2} e_y^{(2)} + K^{3/2}\beta e_y^{(1)} + K^2 B_1 \sin E e_x^{(1)} + \\
&\quad + [\gamma - K^2 B_2 \sin E]\, h_y^{(1)}, \\
e_y^{(2)'} &= -K^{3/2} e_x^{(2)} - K^{3/2}\beta e_x^{(1)} - \gamma h_x^{(1)},
\end{aligned}$$

where

$$\begin{aligned}
K &\triangleq a, \\
A &= [1 + K^2(1 - \cos E)^2]^{-3/2}, \\
B_1 &= 3K(1 - \cos E)A^{5/3}, \\
\gamma &= K^{5/2}(1 - \cos E)(1 - A), \\
\beta &= \tfrac{1}{2} + \Delta'. \\
B_2 &= -3K^{1/2}(\sin E)A^{5/3},
\end{aligned}$$

For the 2nd order approximation an additional equation is needed,

$$\begin{aligned}
e_z^{(2)'} &= [K^{3/2}(1 - \cos E)h_y^{(1)} - K^2 \sin E\, e_x^{(1)} + \\
&\quad + K^{7/2}(1 - \cos E)^2 e_y^{(1)} - K^2(1 - \cos E)^2\, e_x^{(1)'} + \\
&\quad + K^{3/2} \sin E(1 - \cos E)h_y^{(1)'}](1 - A). \quad (3.14)
\end{aligned}$$

The initial state for these equations is at r=0. Periodic orbits are calculated using the fact that $h_y^{(1)}=h_y^{(2)}=e_y^{(1)}=e_y^{(2)}=0$ at any crossing of the

x-z plane of symmetry, i.e., at E=0, π. Solutions of the differential equations in (3.13) and (3.14) can be used in Equation (3.1) to produce $\bar{r}$ which can be compared with the fully integrated results.

It can be noted that the equations in (3.13) are linear. This leads to a simple form for elements of vector $\bar{W}$ at M, the mean anomaly,

$$\bar{W}(M) = \Psi(M, 0)\bar{W}(0) + P(0),$$

where

$$\bar{W} = (h_x^{(1)}, h_y^{(1)}, h_x^{(2)}, h_y^{(2)}, e_x^{(1)}, e_y^{(1)}, e_x^{(2)}, e_y^{(2)})^T.$$

$\Psi(M, 0)$ is the 8x8 transition matrix of the homogeneous equation associated with (3.13), $\partial\bar{W}(t)/\partial\bar{W}(0)$. It is calculated from

$$\frac{d}{dM}\Psi(M, 0) = \bar{\bar{G}}(M)\Psi(M, 0). \tag{3.15}$$

$\Psi(0, 0)=I$ and the 8x8 matrix $\bar{\bar{G}}$ has non-zero elements such that

$$G_{12} = G_{34} = G_{56} = G_{78} = K^{3/2},$$
$$G_{21} = G_{43} = G_{65} = G_{87} = -K^{3/2},$$
$$G_{32} = G_{76} = -G_{41} = -G_{85} = K^{3/2}\beta,$$
$$G_{42} = K^{5/2}(1 - \cos E)B_2,$$
$$G_{45} = -K^{5/2}(1 - \cos E)B_1,$$
$$G_{72} = \gamma - K^2 B_2 \sin E,$$
$$G_{75} = K^2 B_1 \sin E,$$
$$G_{81} = -\gamma.$$

As the vector $\bar{W}$ indicates, ψ is the transition matrix for the 2nd order approximation which contains the 1st order results as well.

The eigenvalues for the 1st order equations can be found in the upper left 2x2 matrix contained in the full cycle $\Psi(M_F, 0)$. The two eigenvalues are always complex conjugates. To evaluate the stability of the periodic orbits produced in the 2nd order case, the 4x4 transition matrix

$$\Gamma(M, 0) = \frac{\partial\bar{Y}(M)}{\partial\bar{Y}(0)}, \tag{3.16}$$

where

$$\bar{Y} = (h_x, h_y, e_x, e_y)^T,$$

is actually needed. But Γ can be calculated from Ψ. It may be assumed that the initial 2nd order variations are always zero, so that the elements of Γ can be calculated according to the following example for element Γ_{12},

$$\frac{\partial h_x(t)}{\partial h_y(0)} = \frac{\partial(\varepsilon h_x^{(1)} + \varepsilon^2 h_x^{(2)})}{\partial(\varepsilon h_y^{(1)} + \varepsilon^2 h_y^{(2)})_0} = \frac{\partial h_x^{(1)}}{\partial h_y^{(1)}}_0 + \frac{\partial h_x^{(2)}}{\partial h_y^{(1)}}_0. \tag{3.17}$$

The four eigenvalues of the matrix Γ can be compared with the eigenvalues found for the fully integrated equations. The stability indices for Γ can be calculated directly as shown previously in Equations (2.4).

4. NUMERICAL RESULTS FOR L_3

Shown in Figures 2a-b, many orbits had previously been calculated in the L_3 family at $\mu=0.96$. Integration of the regularized equations of motion produced additional members of this family located very close to m_2. Initial and final conditions for some representative orbits in this region are shown in Table I. The values for T/2 indicate half the period in units of non-dimensional time. Also shown are the values of the stability indices.

TABLE I: Orbits in the L_3 family at $\mu=0.96$.

x_0^*	0.040096	0.061790	0.120314	0.197908	0.257036	0.350513
z_0	0.422546	1.368386	1.673604	1.778059	1.809052	1.824026
$\dot{y}_0$	-0.005004	-0.036044	-0.081819	-0.140186	-0.185697	-0.256747
T/2	0.311104	1.800978	2.440748	2.692939	2.787250	2.872278
C	4.617555	1.450699	1.192248	1.130949	1.120449	1.128648
ν_1	0.81867	-0.86859	0.28203	0.79518	0.97237	1.13479
ν_2	0.80587	-0.91578	0.11582	0.58190	0.72525	0.83356

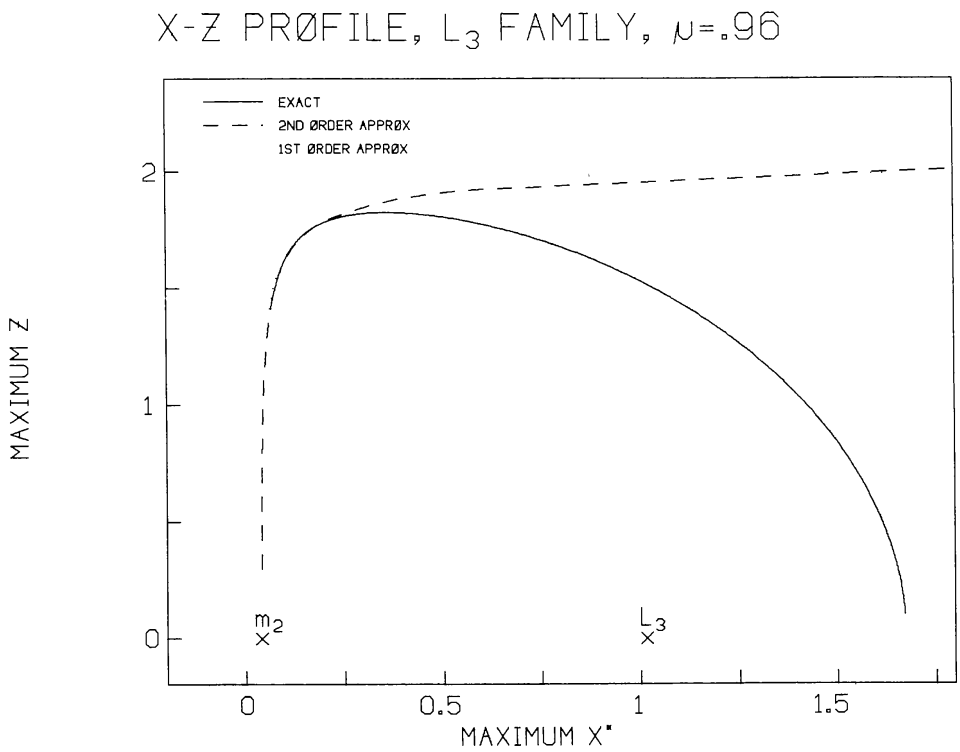

Fig. 4.

It is desired to compare the exact and approximately calculated orbits. The best comparison is made by looking at the family of orbits rather than at individual members. Both integrated and approximate results appear in Figure 4. Here only the x^*_{max}, z_{max} value has been plotted for each orbit.

The solid curve which is the exact result, is the boundary of the x-z projection, part of which is seen in Figure 2a. Note that the z_{max} values drop off quickly after reaching a peak as x_{max} continues to decrease. This is consistent with results at other mass ratios. Results from the 2nd order approximation are seen in the dashed curve. The 1st order result is the dotted curve. Near m_2, only the approximations are shown. They are on the solid curve when it is continued through this area. The 2nd order curve is clearly better at this mass ratio, following the exact curve closely to about $z_{max} \cong 1.8$. This corresponds to $x^*_{max} \cong 0.25$. Even with that difference, however, the 1st order may be preferred because of the very simple form of the equations. Figure 5 indicates the stability of

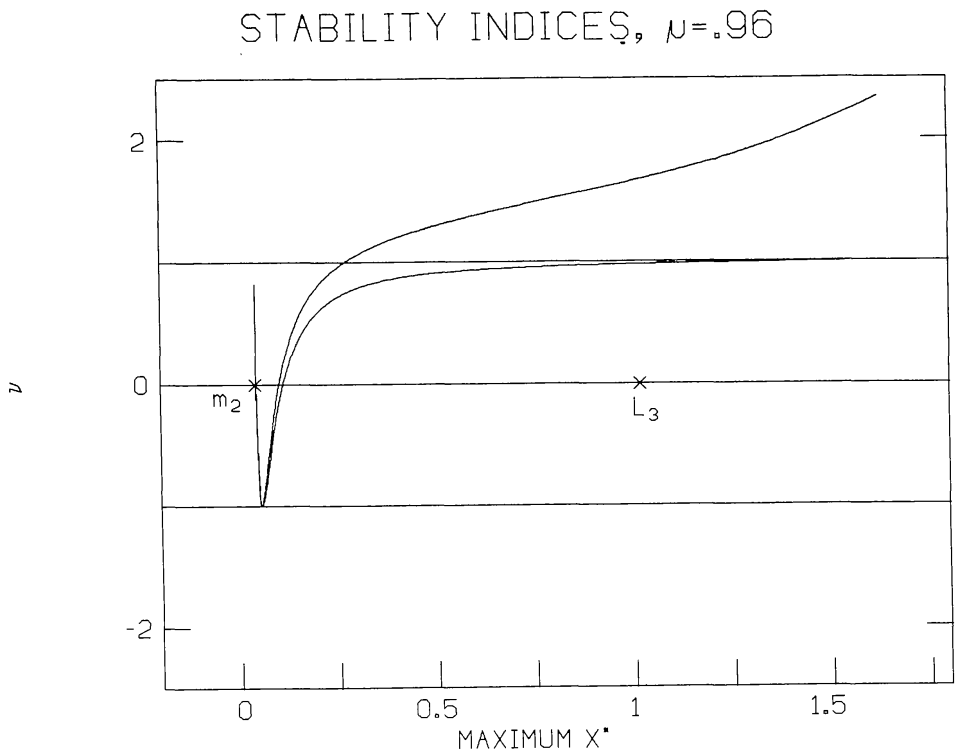

Fig. 5.

members of this family by plotting x^*_{max}, the identifying point for each orbit, versus the stability indices, ν_i. Although none of the orbits is extremely unstable, they are only stable when both ν are between -1 and +1. Difficult to see on this scale, the two ν's do not have quite the same value. Also, as x^*_{max} decreases, both ν appear to pass through -1. Actually one curve dips just below -1, technically outside the sable region. The other curve does not quite reach -1. The almost rectilinear orbits for which the 2nd order approximation is good are almost all contained within the stable region. The ν's both appear to converge to +1 as $z_{max} \to 0$. How well the approximation predicts the stability is shown in Figure 6. Here the portion of Figure 5 in which the approximation is good has been enlarged. The dashed curves are stability indices in the 2nd order case. The 1st order case produces two equal ν and that curve is dotted.

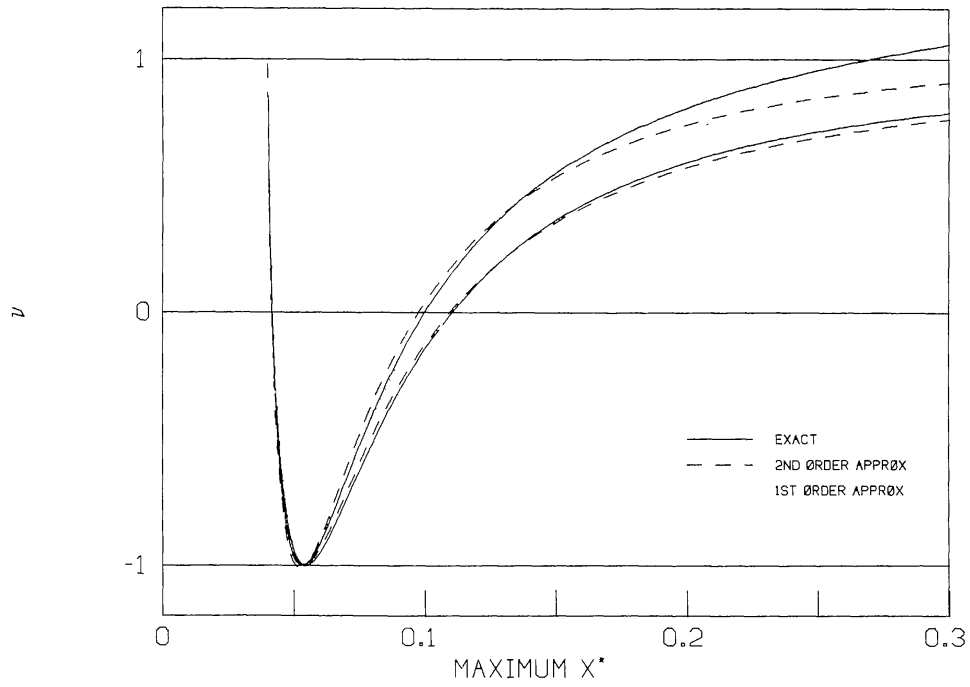

Fig. 6.

Of course, this approximation works best in the region where the initial assumption is valid, i.e., $x, y \ll z$.

As μ is reduced, and ε therefore increased, the approximation is good in a smaller region near the mass. Orbits were both integrated and approximated also at $\mu=0.988$ which corresponds to the L_3 case in the Earth-Moon system. Again a family exists from L_3 to the Earth. However, very close to the point where the ν's dip into the stable range, the orbits dip beneath the surface of the Earth. The outer members of the family are only mildly unstable, much as in Figure 5.

5. APPROXIMATION FOR THE $L_1 - L_2$ BRIDGE FAMILY

In Figure 1, the smaller primary is on the left. For analysis of the almost rectilinear orbits near the smaller primary, the corresponding situation in the equations of motion is choosing μ to be small. When $\mu < 0.5$, the libration point on the far side of $\mu(m_2)$ is then redefined to be L_2. As in the L_3 case, the halo family associated with both L_1 and L_2 tend toward rectilinear orbits as x_{max} is decreased. Breakwell and Brown (1979) presented an analytic approximation to this case for μ very small. The initial assumptions are now $z \ll 1$ and x, y of order z^2_{max}.

Although these are different than those in the L_3 case presented earlier, a similar 1st order analysis can be carried out using some of the variables introduced in Breakwell and Brown (1979).

It is still of interest to analyze the orbit by looking at the in-plane components of the small angular momentum vector and the small in-plane components of the eccentricity vector. To first order, use

$$\bar{h} \cong h_x \hat{x} + h_y \hat{y}, \qquad \bar{e} \cong e_x \hat{x} + e_y \hat{y} - \hat{z}, \tag{5.1}$$

where h_x, h_y, e_x, e_y are small.

Ignoring x, y, $\dot{x}$, $\dot{y}$, the motion is purely one-dimensional, given approximately by

$$\frac{\dot{z}^2}{2} + \frac{z^2}{2} - \frac{\mu}{z} = \text{constant} = \frac{z_{max}^2}{2} - \frac{\mu}{z_{max}} . \tag{5.2}$$

Introducing $\eta = 1 - 2\mu/z_{max}^3$ and $\zeta = z/\mu^{1/3}$, $\zeta_M = z_{max}/\mu^{1/3}$, and $u = \zeta/\zeta_M$, rewrite it as

$$\dot{\zeta}^2 = \frac{\zeta_M^2}{u}(1 - u)(1 - \eta + u + u^2). \tag{5.3}$$

Also introducing $S = -(\text{sgn } \dot{z})\sqrt{1-u}$,

$$\dot{S} = \frac{R}{2\sqrt{u}} ,$$

where $R = \sqrt{1-\eta+u+u^2}$. This permits the introduction of S as the independent variable in place of time, which is determined by a quadrature. Now the perturbation due to the other primary, seen in (3.9), can be written in another form (with μ small) as

$$\bar{f}_1 = (3\hat{x}\hat{x}^T - 1)\bar{r} + \frac{3}{2} z^2 \hat{x}. \tag{5.4}$$

The approximation for $\bar{r}$ in (3.1) in another form is

$$\bar{r} \cong z\left(\frac{\dot{z}}{\mu}\hat{z} \times \bar{h} - e_x \hat{x} - e_y \hat{y} + \hat{z}\right). \tag{5.5}$$

Using these in (3.12), obtain

$$\dot{\bar{h}} \cong -3z^2\left(e_x + \frac{\dot{z}}{\mu} h_y\right)\hat{y} + \frac{3}{2} z^3 \hat{y}, \tag{5.6}$$

$$\dot{\bar{e}} \cong \frac{3z^2\dot{z}}{\mu}\left(e_x + \frac{\dot{z}}{\mu} h_y\right)\hat{x} + \frac{z}{\mu}(h_y \hat{x} - h_x \hat{y}) - \frac{3}{2}\frac{z^3\dot{z}}{\mu}\hat{x}.$$

Next it is convenient to eliminate the small parameter μ by scaling according to

$$h_x \hat{x} + h_y \hat{y} = \mu(\lambda_x \hat{x} + \lambda_y \hat{y}), \qquad e_x \hat{x} + e_y \hat{y} = \mu^{1/3}(\varepsilon_x \hat{x} + \varepsilon_y \hat{y}). \tag{5.7}$$

Hence, the scalar equations in the new scaled variables are

$$\begin{aligned}
\dot{\lambda}_x &= \lambda_y, \\
\dot{\lambda}_y &= -\lambda_x + \frac{3\zeta^2\zeta_M SR}{\sqrt{u}}\lambda_y - 3\zeta^2\varepsilon_x + \frac{3}{2}\zeta^3, \\
\dot{\varepsilon}_x &= \varepsilon_y + \left(\zeta + 3\zeta^2\zeta_M^3\frac{S^2R^2}{u}\right)\lambda_y - \frac{3\zeta^2\zeta_M SR}{\sqrt{u}}\varepsilon_x + \frac{3}{2}\frac{\zeta^3\zeta_M SR}{\sqrt{u}}, \\
\dot{\varepsilon}_y &= -\varepsilon_x - \zeta\lambda_x.
\end{aligned} \tag{5.8}$$

Desiring to use S as the independent variable introduce the 4-vector $X = (\lambda_x\lambda_y\varepsilon_x\varepsilon_y)^T$. Use

$$\frac{dX}{dS} = \bar{\bar{A}}(S)X + \bar{B}(S), \tag{5.9}$$

where the non-zero elements of the 4x4 matrix $\bar{\bar{A}}$ and the vector $\bar{B}$ are

$$A_{12} = A_{34} = -A_{21} = -A_{43} = 2\sqrt{u}/R,$$

$$A_{41} = \zeta A_{21}, \qquad A_{33} = \zeta A_{12} + 6\zeta\zeta_M^3 S^2 R\sqrt{u},$$

$$A_{22} = -A_{33} = 6\zeta^2\zeta_M S, \qquad A_{23} = -6\zeta^2\sqrt{u}/R,$$

$$B_2 = 3\zeta^3\sqrt{u}/R, \qquad B_3 = 3\zeta^3\zeta_M S.$$

The periodic halo orbits again have ε_y and λ_y zero at intersections with the x-z plane, i.e., at S = -1 and S = 0. This determines ε_x and λ_x at S = -1 (closest to the small primary) as well as at S = 0.

The stability is determined by the eigenvalues of the full-cycle transition matrix $\Phi(1, -1)$ from S = -1 to S = +1. Here $\Phi(-1, -1) = I$ and

$$\frac{d}{dS}\Phi(S, -1) = \bar{\bar{A}}(S)\Phi(S, -1). \tag{5.10}$$

These 4 eigenvalues are again in pairs $(\lambda_i, 1/\lambda_i)$, since the equations are invariant under $S \to -S$, $\lambda_y \to -\lambda_y$, $\varepsilon_y \to -\varepsilon_y$. The stability indices are calculated as before from (2.4). Equations equivalent to (5.8), with slightly different dependent variables and a more laborious derivation, were given in Breakwell and Brown (1979). The stability indices ν_1, ν_2 as functions of ζ_M were identical with those obtained here.

6. NUMERICAL RESULTS FOR THE $L_1 - L_2$ BRIDGE FAMILY

Being considered are almost rectilinear orbits near the smaller primary. They can be on either side of m_2, in either the L_1 or L_2 family. Orbits were calculated with the Earth-Moon mass ratio $\mu = 0.012$ for comparison with results obtained by Breakwell and Brown. The results are identical.

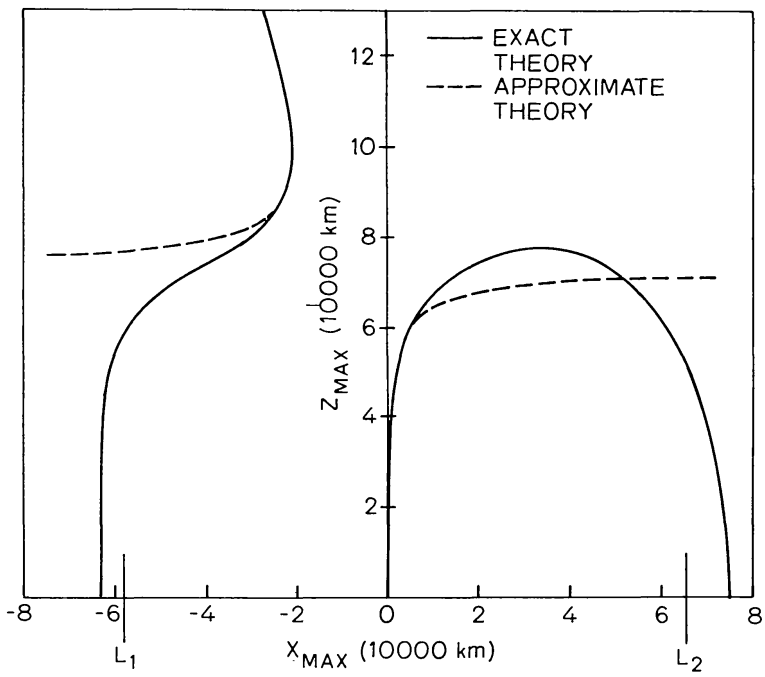

Fig. 7. The halo family Apolune points.

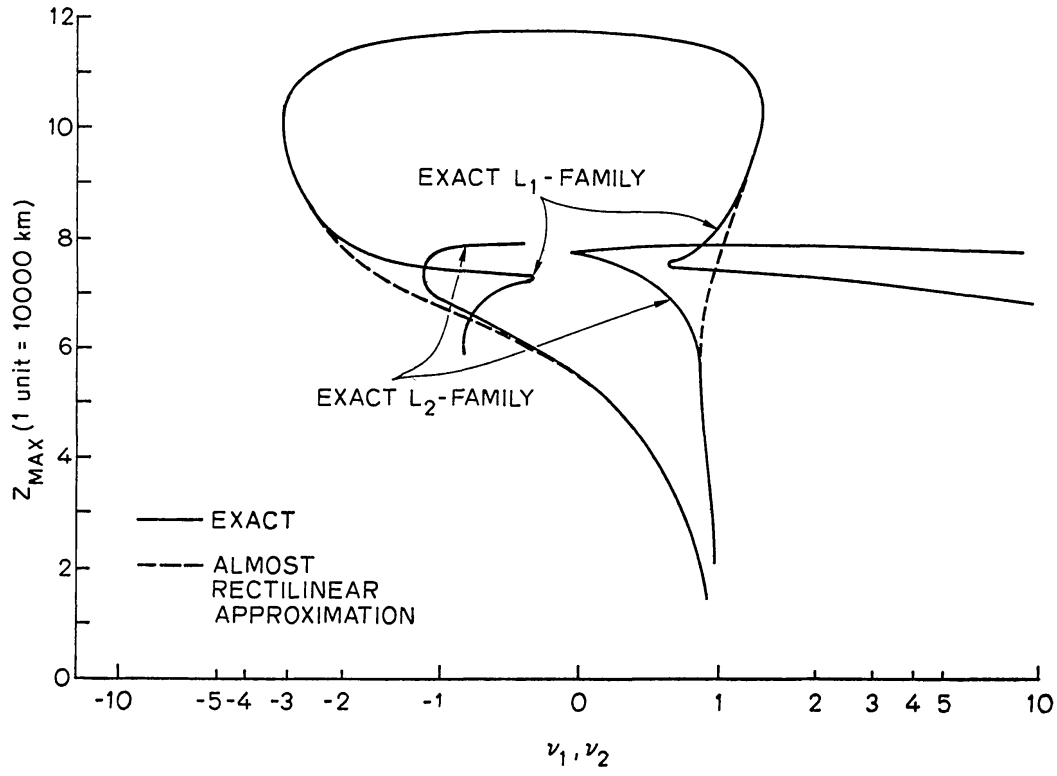

Fig. 8.

Figure 7 shows the exact apolune points for the L_1 and L_2 halo family in the Earth-Moon case, as well as the almost rectilinear approximation. Figure 8 shows the stability indices ν_i for the same problem, the approximation forming a bridge between the two families.

The orbits are found to be stable for $\zeta_M < 0.761$, at which value one of the ν's reaches -1. At $\zeta_M = 0.832$, the other ν reaches +1 and the corresponding initial small parameters $(\lambda_x)_0$ and $(\varepsilon_x)_0$ approach $+\infty$ and $-\infty$, respectively, indicating a complete breakdown in the approximation. However, for $\zeta_M > 0.832$, the initial small parameters are again finite and with reversed signs. This second branch approximates the L_1 halo family, while the earlier branch ($\zeta_M < 0.832$) approximates the L_2 halo family. At $\zeta_M = 1.310$ the orbits again become stable (both ν's less than 1), the positive ν having in fact already passed below +1 at $\zeta_M = 1.2815$, without however any divergence of the initial small parameters. The stability is however short-lived, since above $\zeta_M = 1.3186$ the ν's become complex, being both -0.192 at this ζ_M.

7. CONCLUSIONS

The halo orbits originating in the neighborhood of either L_1 or L_2 near the smaller primary, or of L_3, near the larger primary, tend toward almost rectilinear orbits perpendicular to the plane of motion of the primaries as the halo orbit moves away from the libration point toward the nearer primary.

These almost rectilinear orbits can be approximated by one of the two linear analyses, depending on whether μ or $(1 - \mu)$ is small. The linear analysis also gives a satisfactory account of the stability of the orbits in question.

APPENDIX A

A1. Regularization of the Restricted Three-Body Problem in the Rotating Frame

This derivation is very similar to that shown in Bettis and Szebehely (1971) for a more general problem in a nonrotating frame. Begin with the equations of motion, written in the original variables from Section 2 as

$$\begin{aligned} \ddot{x} - 2\dot{y} &= \frac{\partial U}{\partial x}, \\ \ddot{y} + 2\dot{x} &= \frac{\partial U}{\partial y}, \\ \ddot{z} &= \frac{\partial U}{\partial z}, \end{aligned} \tag{A1.1}$$

where

$$U = \frac{1}{2}(x^{*2} + y^2) + \frac{1 - \mu}{d} + \frac{\mu}{r},$$

$x^* = x + 1 - \mu$, d = distance from m_1, r = distance from m_2.

The constant C, is given by

$$\frac{\dot{x}^2 + \dot{y}^2 + \dot{z}^2}{2} = U - \frac{C}{2} . \tag{A1.2}$$

Regularization involves first, the transformation of the independent variable, t, and second, the transformation of the coordinates x, y, z. The time transformation is defined by

$$dt = r\, d\tau, \tag{A1.3}$$

to the new independent variable τ. The equations (A.1) now appear as

$$\begin{aligned} x'' - 2ry' &= \frac{x'}{r^2}(\bar{r}\cdot\bar{r}') - \frac{\mu x}{r} + r^2 F_1, \\ y'' + 2rx' &= \frac{y'}{r^2}(\bar{r}\cdot\bar{r}') - \frac{\mu y}{r} + r^2 F_2, \\ z'' &= \frac{z'}{r^2}(\bar{r}\cdot\bar{r}') - \frac{\mu z}{r} + r^2 F_3, \end{aligned} \tag{A1.4}$$

where

$$\begin{aligned} \bar{r}\cdot\bar{r}' &= xx' + yy' + zz', \\ F_1 &= -\frac{(1-\mu)(1+x)}{d^3} + (1-\mu) + x, \\ F_2 &= -\frac{(1-\mu)y}{d^3} + y, \\ F_3 &= -\frac{(1-\mu)z}{d^3} . \end{aligned}$$

Prime indicates differentiation with respect to τ.

The coordinate transformation is from the position variables x, y, z to the new variables u_1, u_2, u_3, and u_4. To move from a three-dimensional representation to one in four dimensions, it is convenient to define the four-dimensional column vectors

$$\begin{aligned} \bar{R} &= (x, y, z, 0)^T, \\ \bar{R}' &= (x', y', z', 0)^T, \\ \bar{u} &= (u_1, u_2, u_3, u_4)^T. \end{aligned}$$

Then the equations in (A1.4) can be written in a four-dimensional matrix form as

$$\bar{R}'' = \frac{\bar{R}\cdot\bar{R}'}{\bar{R}\cdot\bar{R}}\bar{R}' + r\bar{\bar{B}}\bar{R}' - \mu\frac{\bar{R}}{R} + r^2\bar{F}, \tag{A1.5}$$

where

$$R = |\bar{R}|,$$

$$\bar{\bar{B}} = \begin{pmatrix} 0 & 2 & 0 & 0 \\ -2 & 0 & 0 & 0 \\ 0 & 0 & 0 & 0 \\ 0 & 0 & 0 & 0 \end{pmatrix},$$

$$\bar{F} = (F_1, F_2, F_3, 0)^T.$$

This equation is still written in the rotating coordinate system. Numerical problems for orbits in which r, or equivalently R, approaches zero can be seen since that variable appears in the denominator.

To effect the coordinate transformation use the relation

$$\bar{R} = \mathfrak{L}(\bar{u})\bar{u}, \tag{A1.6}$$

where

$$\mathfrak{L}(\bar{u}) = \begin{pmatrix} u_1 & -u_2 & -u_3 & u_4 \\ u_2 & u_1 & -u_4 & -u_3 \\ u_3 & u_4 & u_1 & u_2 \\ u_4 & -u_3 & u_2 & -u_1 \end{pmatrix}.$$

It can be shown that $r = \bar{u}\cdot\bar{u}$. The operator $\mathfrak{L}(\bar{u})$ has the following properties:

(1) $\mathfrak{L}^T(\bar{u})\,\mathfrak{L}(\bar{u}) = rI$.

(2) $\mathfrak{L}'(\bar{u}) = \mathfrak{L}(\bar{u}')$.

(3) $\mathfrak{L}(\bar{u})\bar{u}' = \mathfrak{L}(\bar{u}')\bar{u} = \frac{1}{2}\bar{R}'$ assuming that the derivatives of the new variables u_i satisfy an additional condition that

$$u_4u_1' - u_3u_2' + u_2u_3' - u_1u_4' = 0.$$

(4) $(\bar{u}\cdot\bar{u})\mathfrak{L}(\bar{u}')\bar{u}' - 2(\bar{u}\cdot\bar{u}')\mathfrak{L}(\bar{u})\bar{u}' + (\bar{u}'\cdot\bar{u}')\mathfrak{L}(\bar{u})\bar{u} = 0.$

Further differentiation of $\bar{R}'$ in Property (3) and application of Property (2) provides the useful relationship

$$\bar{R}'' = 2\mathfrak{L}(\bar{u})\bar{u}'' + 2\mathfrak{L}(\bar{u}')\bar{u}'. \tag{A1.7}$$

Using (A1.6), Property (3) and (A1.7), the matrix equation in (A1.5) becomes

$$(\bar{u}\cdot\bar{u})\mathfrak{L}(\bar{u})\bar{u}'' + (\bar{u}\cdot\bar{u})\mathfrak{L}(\bar{u}')\bar{u}' = 2(\bar{u}\cdot\bar{u}')\mathfrak{L}(\bar{u})\bar{u}' +$$

$$+ (\bar{u}\cdot\bar{u})^2\bar{\bar{B}}\mathfrak{L}(\bar{u})\bar{u}' - \frac{\mu}{2}\mathfrak{L}(\bar{u})\bar{u} + \frac{(\bar{u}\cdot\bar{u})^3}{2}\bar{F}. \tag{A1.8}$$

Applying Property (4) of the operator $\mathfrak{L}$ produces

$$\mathfrak{L}(\bar{u})\bar{u}'' - \frac{(\bar{u}'\cdot\bar{u}')}{(\bar{u}\cdot\bar{u})}\mathfrak{L}(\bar{u})\bar{u} = (\bar{u}\cdot\bar{u})\bar{\bar{B}}\mathfrak{L}(\bar{u})\bar{u}' - \frac{\mu}{2}\frac{\mathfrak{L}(\bar{u})\bar{u}}{(\bar{u}\cdot\bar{u})} +$$

$$+ \frac{(\bar{u}\cdot\bar{u})^2}{2}\bar{F}. \tag{A1.9}$$

From Property (1), the inverse of the operator can be defined $\mathfrak{L}^{-1}(\bar{u}) = \mathfrak{L}^T(\bar{u})/(\bar{u}\cdot\bar{u})$. Multiply by the inverse and rearrange Equation (A1.9) for a

more useful form

$$\bar{u}'' + \frac{\mu - 2(\bar{u}'\cdot\bar{u}')}{2(\bar{u}\cdot\bar{u})}\bar{u} = \mathfrak{L}^T(\bar{u})\bar{\bar{B}}\mathfrak{L}(\bar{u})\bar{u}' + \frac{(\bar{u}\cdot\bar{u})}{2}\mathfrak{L}^T(\bar{u})\bar{F}. \tag{A1.10}$$

The second term of (A1.10) still contains $(\bar{u}\cdot\bar{u}) = r$ in the denominator. However, a new variable h can be introduced and defined such that

$$h = \frac{(\dot{\bar{R}}\cdot\dot{\bar{R}})}{2} - \frac{\mu}{R}, \tag{A1.11}$$

or equivalently

$$h = \frac{2\mathfrak{L}(\bar{u})\bar{u}'\cdot\mathfrak{L}(\bar{u})\bar{u}'}{r^2} - \frac{\mu}{r}. \tag{A1.12}$$

From linear algebra

$$\mathfrak{L}(\bar{u})\bar{u}'\cdot\mathfrak{L}(\bar{u})\bar{u}' = \bar{u}'\cdot\mathfrak{L}^T(\bar{u})\mathfrak{L}(\bar{u})\bar{u}'. \tag{A1.13}$$

Using (A1.13) and Property (1), h can also be defined as

$$h = \frac{2(\bar{u}'\cdot\bar{u}') - \mu}{(\bar{u}\cdot\bar{u})}, \tag{A1.14}$$

which is very similar to the second term of (A1.10). Replace that term by $-(h/2)\bar{u}$ and calculate h using (A1.11). $(\dot{\bar{R}}\cdot\dot{\bar{R}})$ is the square of the velocity in the rotating frame which has been related to $\bar{R}$ through the constant in (A1.12). The result is

$$\bar{u}'' - \frac{h}{2}\bar{u} = \mathfrak{L}^T(\bar{u})\bar{\bar{B}}\mathfrak{L}(\bar{u})\bar{u}' + \frac{(\bar{u}\cdot\bar{u})}{2}\mathfrak{L}^T(\bar{u})\bar{F}, \tag{A1.15}$$

where

$$h = \frac{1-\mu}{d} + \frac{1}{2}(x^{*2} + y^2) - \frac{C}{2},$$

which contains no singularities.

The 6x6 transition matrix, $\Phi(t, 0)$, as seen in Section 2, cannot be transformed directly to remove all singularities. Rather an 8x8 transition matrix, $\Psi(\tau, 0)$, associated with the u's can be calculated where $\Psi(\tau, 0) = \partial Y(\tau)/\partial Y(0)$ and $Y = (u_1, u_2, u_3, u_4, u_1', u_2', u_3', u_4')^T$. As usual $\Psi(0, 0) = I$ and

$$\frac{d}{d\tau}\Psi(\tau, 0) = \bar{\bar{A}}(\tau)\Psi(\tau, 0), \tag{A1.16}$$

where $\bar{\bar{A}}(\tau)$ is an 8x8 matrix defined by

$$\bar{\bar{A}} = \left(\begin{array}{c|c} 0 & I \\ \hline G & H \end{array}\right),$$

$$G_{ij} = \frac{\partial u_i''}{\partial u_j}, \quad i, j = 1, 2, 3, 4,$$

$$H_{ij} = \frac{\partial u_i''}{\partial u_j'}, \quad i, j = 1, 2, 3, 4.$$

Matrices $\bar{\bar{G}}$ and $\bar{\bar{H}}$ are determined using the forms of u_i'' shown in (A1.15).

The system of equations to be integrated then consists of the independent variable transformation in (A1.13), the 8 first order equations in (A1.15), and the 64 equations for Ψ in (A1.16) for a total of 73.

A2. Finding Periodic Orbits

For the desired simply symmetric orbits the initial vector appears as

$$X_0 = (x_0, 0, z_0, 0, \dot{y}_0, 0)^T, \tag{A2.1}$$

indicating a perpendicular departure from the x-z plane. By introducing the 4th dimension, one of the initial u's may be arbitrarily chosen. Here $u_{4_0} = 0$ was selected so that the transformed initial vector appears as

$$Y_0 = (u_{1_0}, 0, u_{3_0}, 0, 0, u_{2_0}', 0, u_{4_0}')^T. \tag{A2.2}$$

As before, integration continues until the next crossing of the x-z plane at $y = 2(u_1u_2 - u_3u_4) = 0$. For integration purposes, $t_F/2$ is defined to occur when $|y| < 10^{-11}$. The exact initial conditions for periodicity are not known so the second crossing of the x-z plane may not be perpendicular. This is tested using two values

$$\begin{aligned} v_1 &= u_1u_1' - u_2u_2' - u_3u_3' + u_4u_4', \\ v_2 &= u_1u_3' + u_2u_4' + u_3u_1' + u_4u_2', \end{aligned} \tag{A2.3}$$

since $\dot{x} = 2v_1/R$ and $\dot{z} = 2v_2/R$. The orbit is considered 'periodic' when $|v_1|, |v_2| < 10^{-8}$. If this is not the case, corrections to the initial vector Y_0 can be calculated using $\Psi(\tau_F/2, 0)$. The desired changes in the end values at $\tau_F/2$, $-v_1$ and $-v_2$, need to be produced by changes in the initial conditions. The changes in end conditions are described by the variation of (A2.3) as

$$\begin{aligned} &u_{1_E}\delta u_{1_E}' + u_{1_E}'\delta u_{1_E} - u_{2_E}\delta u_{2_E}' - u_{2_E}'\delta u_{2_E} - u_{3_E}\delta u_{3_E}' - \\ &\quad - u_{3_E}'\delta u_{3_E} + u_{4_E}\delta u_{4_E}' + u_{4_E}'\delta u_{4_E} = -v_1, \\ &u_{1_E}\delta u_{3_E}' + u_{3_E}'\delta u_{1_E} + u_{2_E}\delta u_{4_E}' + u_{4_E}'\delta u_{2_E} + u_{3_E}\delta u_{1_E}' + \\ &\quad + u_{1_E}'\delta u_{3_E} + u_{4_E}\delta u_{2_E}' + u_{2_E}'\delta u_{4_E} = -v_2. \end{aligned} \tag{A2.4}$$

Knowing the vector $Y_E = Y(\tau_F/2)$ it is necessary to describe the end variations

in terms of initial variations. These are

$$\delta Y_E = \psi(\tau_F/2, 0)\delta Y_0 + \frac{\partial Y}{\partial \tau} \delta(\tau_F/2), \tag{A2.5}$$

where

$$\delta Y_0 = (\delta u_{1_0}, 0, \delta u_{3_0}, 0, 0, \delta u'_{2_0}, 0, \delta u'_{4_0})^T.$$

and $\delta Y/\delta\tau$ is evaluated at $\tau_F/2$. The variation $\delta(\tau_F/2)$ is determined by using the fact that the value $y = 0$ does not change at $\tau_F/2$ or

$$\delta y = 2(u_{2_E}\delta u_{1_E} + u_{1_E}\delta u_{2_E} - u_{4_E}\delta u_{3_E} - u_{3_E}\delta u_{4_E}) = 0. \tag{A2.6}$$

The first four equations in (A2.5) are substituted for δu_{i_E} and (A2.6) is solved for $\delta(\tau_F/2)$.

Because there are four initial values to correct, two additional equations must be added to (A2.4). First, the value C remains constant along any solution. Rewrite equation (A1.2) in terms of the new coordinates and vary it in such a way that C remains unchanged, so that

$$2(u'_{2_0}\delta u'_{2_0} + u'_{4_0}\delta u'_{4_0}) = (u_{1_0}\delta u_{1_0} + u_{3_0}\delta u_{3_0})\left(U^*_0 - \frac{C}{2}\right) + \frac{(u^2_{1_0} + u^2_{3_0})}{2}\left(\frac{\partial U^*_0}{\partial u_{1_0}}\delta u_{1_0} + \frac{\partial U^*_0}{\partial u_{3_0}}\delta u_{3_0}\right), \tag{A2.7}$$

where

$$U^*_0 = \frac{1-\mu}{d_0} + \frac{1}{2}x^{*2}_0 .$$

Second, vary an equation from Property (3) of $\mathfrak{L}(\bar{u})$ to produce

$$u_{3_0}\delta u'_{2_0} + u_{1_0}\delta u'_{4_0} = -u'_{4_0}\delta u_{1_0} - u'_{2_0}\delta u_{3_0}. \tag{A2.8}$$

A3. Derivation of Matrix $\mathfrak{M}$ to Evaluate Stability

Once a periodic orbit is obtained, the second half of the orbit must be integrated to obtain the full-cycle 8x8 transition matrix, $\psi(\tau_F, 0)$. However, from $\psi(\tau_F, 0)$, the 4x4 matrix $\mathfrak{M}$ can be derived to give the 4 critical eigenvalues such that

$$\begin{pmatrix} dx_F \\ dz_F \\ d\dot{x}_F \\ d\dot{z}_F \end{pmatrix} = \mathfrak{M} \begin{pmatrix} \delta x_0 \\ \delta z_0 \\ \delta \dot{x}_0 \\ \delta \dot{z}_0 \end{pmatrix}, \tag{A3.1}$$

$\mathfrak{M}$ was derived in the original system by supposing that x_0, z_0, $\dot{x}_0$, $\dot{z}_0$ but not y_0 are varied. This corresponds to adding $\delta u'_{1_0}$, $\delta u'_{3_0}$ to the possible variations in the previous section.

The term on the left in (A3.1) can also be written

$$\begin{pmatrix} dx_F \\ dz_F \\ d\dot{x}_F \\ d\dot{z}_F \end{pmatrix} = 2 \left(\begin{array}{c|c} I & 0 \\ \hline 0 & T \end{array}\right) \left(\begin{array}{c|c} S & 0 \\ \hline S' & S \end{array}\right) \delta Y_F, \tag{A3.2}$$

where

$$I = \begin{pmatrix} 1 & 0 \\ 0 & 1 \end{pmatrix},$$

$$T = \begin{pmatrix} 1/R & 0 \\ 0 & 1/R \end{pmatrix},$$

$$S = \begin{pmatrix} u_{1F} & -u_{2F} & -u_{3F} & u_{4F} \\ u_{3F} & u_{4F} & u_{1F} & u_{2F} \end{pmatrix},$$

$$S' = \begin{pmatrix} u'_{1F} & -u'_{2F} & -u'_{3F} & u'_{4F} \\ u'_{3F} & u'_{4F} & u'_{1F} & u'_{2F} \end{pmatrix},$$

$$\delta Y_F = (\delta u_{1F}, \delta u_{2F}, \delta u_{3F}, \delta u_{4F}, \delta u'_{1F}, \delta u'_{2F}, \delta u'_{3F}, \delta u'_{4F})^T.$$

δY_F can again be described by (A2.5) but now

$$\delta Y_0 = (\delta u_{1_0}, 0, \delta u_{2_0}, 0, \delta u'_{1_0}, \delta u'_{2_0}, \delta u'_{3_0}, \delta u'_{4_0})^T.$$

A new value of $\delta(\tau_F/2)$ can again be defined in terms of the elements of δY_0 by using (A2.6). Next, since $u'_{1_0} = u'_{3_0}$ is still true, (A2.7) remains valid and can be used to write $\delta u'_{2_0}$ and $\delta u'_{4_0}$ in terms of δu_{1_0} and δu_{3_0}. After the above manipulations, (A3.2) appears in the form

$$\begin{pmatrix} dx_F \\ dz_F \\ d\dot{x}_F \\ d\dot{z}_F \end{pmatrix} = P \begin{pmatrix} \delta u_{1_0} \\ \delta u_{3_0} \\ \delta u'_{1_0} \\ \delta u'_{3_0} \end{pmatrix}, \tag{A3.3}$$

with the 4x4 matrix P. But it can also be shown that

$$\begin{pmatrix} \delta u_{1_0} \\ \delta u_{3_0} \\ \delta u'_{1_0} \\ \delta u'_{3_0} \end{pmatrix} = N \begin{pmatrix} \delta x_0 \\ \delta z_0 \\ \delta \dot{x}_0 \\ \delta \dot{z}_0 \end{pmatrix}, \tag{A3.4}$$

where

$$N = \frac{1}{2(u_{1_0}^2 + u_{3_0}^2)} \left(\begin{array}{c|c} Q & 0 \\ \hline 0 & Q \end{array}\right)\left(\begin{array}{c|c} I & 0 \\ \hline 0 & T^{-1} \end{array}\right),$$

$$Q = \begin{pmatrix} u_{1_0} & u_{3_0} \\ -u_{3_0} & u_{1_0} \end{pmatrix},$$

$$T^{-1} = \begin{pmatrix} R & 0 \\ 0 & R \end{pmatrix}.$$

Although calculation of P is certainly not trivial, from here it is apparent that

$$\mathfrak{M} = PN. \tag{A3.5}$$

In comparisons made, this matrix $\mathfrak{M}$ was found to correspond very well with the matrix from the original set of equations.

REFERENCES

Bettis, D. G. and Szebehely, V.: 1971, 'Treatment of Close Approaches in the Numerical Integration of the Gravitational Problem of N Bodies', Astrophys. Space Sci. 14, 133.

Breakwell, J. V. and Brown, J. V.: 1979, 'The "Halo" Family of 3-Dimensional Periodic Orbits in the Earth-Moon Restricted 3-Body Problem', Celest. Mech. 20, 389.

Broucke, R.: 1969, 'Stability of Periodic Orbits in the Elliptic, Restricted Three-Body Problem', AIAA Journal 7, 1003.

Farquhar, R. W. and Kamel, A. A.: 1973, 'Quasi-Periodic Orbits About the Translunar Libration Point', Celest. Mech. 7, 458.

Howell, K. C.: 1984, 'Three-Dimensional, Periodic, "Halo" Orbits', Celest. Mech. 32, 53 (this issue).

Kustaanheimo, P. and Stiefel, E.: 1965, 'Perturbation Theory of Kepler Motion Based on Spinor Regularization', Journal für die reine und angewandte Mathematik 218, 204.